

SUPPLEMENTARY INFORMATION:

high-performance cavity-enhanced quantum memory with warm atomic cell

Lixia Ma^{1,3}, Xing Lei^{1,3}, Jielu Yan¹, Ruiyang Li¹, Ting Chai¹, Zhihui Yan^{1,2*}, Xiaojun Jia^{1,2†}, Changde Xie^{1,2} & Kunchi Peng^{1,2}

¹State Key Laboratory of Quantum Optics Quantum Optics Devices, Institute of Opto-Electronics, Shanxi University, Taiyuan 030006, P. R. China

²Collaborative Innovation Center of Extreme Optics, Shanxi University, Taiyuan 030006, P. R. China

³These authors contributed equally: Lixia Ma, Xing Lei.

*e-mail:zhyan@sxu.edu.cn

†e-mail:jiaxj@sxu.edu.cn

In the following, we provide additional information on high-performance cavity-enhanced quantum memory with warm atomic cell. In Supplementary Note 1, we discuss the experimental details. In Supplementary Note 2, the time sequence of cavity-enhanced quantum memory is shown. In Supplementary Note 3, we study theoretical analyze of cavity-enhanced quantum memory. In Supplementary Note 4, we investigate the memory fidelity of cavity-enhanced quantum memory.

Supplementary Note 1 - Experimental details

The experimental setup for cavity-enhanced quantum memory is shown in Fig. 1 (b). A ⁸⁷Rb atomic cell with 3 mm diameter and 10 mm length is filled with 10 torr of neon buffer gas to slow the atomic diffusion and reduce the time-of-flight broadening. The atomic cell is placed in a bow tie-type ring cavity with the length of 486 mm and finesse of 17. A Ti:sapphire laser (Coherent MBR-110) pumped by green laser (Yuguang DPSS FG-VIIB) outputs 3 W laser with coherent state, which is divided into three parts: the first part is injected into the cavity-enhanced quantum memory which is utilized as signal mode, the second part is frequency shifted and power amplified which is used as control mode of quantum memory system, and the last part is the local oscillation of time-domain balanced homodyne detector (BHD).

The Pound-Drever Hall technique for cavity locking is implemented by using photoreceiver detector D2 to measure the transmitted optical mode after the Glan-Thompson polarizer P3. The spatial mode matching efficiency is 99%. An approximate exponential growth wave packet with the time constant of 50 ns to match the cavity-enhanced memory mode is used as the input signal

mode of quantum memory, which is dynamically shaped in time by an electro-optical amplitude modulator (EOAM), and taken as the time reversed version of cavity-enhanced quantum memory to provide the optimum coupling. The control mode frequency shift of 6.8 GHz is realized by the electro-optical phase modulator (EOPM), and its power is amplified through the laser amplifier. The frequencies of both signal and control optical modes are red detuned by $\Delta_s = 700$ MHz (the detuning of signal optical modes from the transition between energy levels $|5S_{1/2}, F = 1\rangle$ and $|5P_{1/2}, F' = 1\rangle$) and $\Delta_c = 700.5$ MHz (the detuning of control optical mode from the transition between energy levels $|5S_{1/2}, F = 2\rangle$ and $|5P_{1/2}, F' = 1\rangle$), respectively.

The Glan-Thompson polarizers P1 and P2 are applied to couple or separate signal and control modes. The signal mode with a horizontal polarization, which can pass through two polarizers P1 and P2, is used as the input signal mode of memory system and injected into the measurement system. Meanwhile, the control mode with a vertical polarization is reflected into the memory system by the polarizer P1. In the system the output control mode will be filtered by a polarizer P2 and a series of etalons, and thus only the signal modes are measured by photoreceiver detector D1 and BHD, respectively. While the foldable mirror M5 is removed, and the input signal mode was generated by modulating the continuous-wave coherent light with the power level of $50\ \mu\text{W}$, the photon fluxes of input and stored-and-retrieved signal modes are measured by photoreceiver detector D1. When the leakage and stored-and-retrieved signal modes are reflected by the foldable mirror M5, their quadrature components with single photon level are measured by BHD. The stored-and-retrieved signal mode with the total transmission efficiency of 86% is measured. 86% of the stored-and-retrieved signal mode and 14% of vacuum state resulting from transmission loss are coupled into BHD to measure the quadrature components, which means 14% overlap of a weak coherent state with the vacuum state.

Supplementary Note 2 - Time sequence of cavity-enhanced quantum memory

The input and stored-and-retrieved signal modes are measured respectively at different time and thus can be distinguished. Before quantum memory, the photon flux of an input signal mode is measured and shown in the red line of Fig. 2 (a). Quantum memory includes the writing ($t < 0$), storage ($0 < t < 100\text{ns}$) and reading ($t > 100\text{ns}$) process. In the quantum memory, the photon fluxes of the leakage and the stored-and-retrieved signal modes are measured and shown as the blue line in Fig. 2 (a). When $t < 0$, both the weak signal and the strong control modes

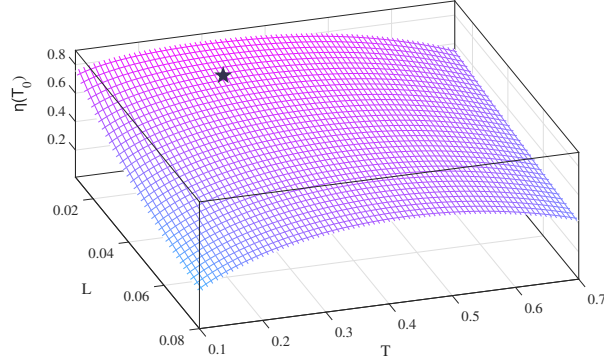


FIG. S1: The dependence of memory efficiency $\eta(T_0)$ on the transmissivity of the input-output mirror T and the intracavity loss L . The black star corresponds the experimentally measured result.

interact with an atomic medium, and the input signal is stored in the atomic medium. However, in this process there is always a modest part of injected mode to be leaked which will be measured. The lifetime defined as a $1/e$ coherence time is $1.2 \mu\text{s}$, and the storage time T_0 is controlled by user within the lifetime. As $0 < t < T_0$, the quantized state of light is stored and preserved in atom ensemble. At $t > 100\text{ns}$, the optical mode is retrieved from atomic medium and measured. The control mode is switched by a pair of acousto-optical modulators (AOMs) to implement the user-controlled quantum memory.

Supplementary Note 3 - Theoretical analyze of cavity-enhanced quantum memory

To discuss the performance of cavity-enhanced quantum memory, Fig. S1 shows that the dependence of memory efficiency on the transmissivity of the input-output mirror T and the intracavity loss L for the storage time of 100 ns. All parameter values are experimentally reachable to provide direct references for experimental system design, where the effective light-atom coupling constant κ is 59 MHz and the spin wave decoherence rate γ_0 is 420 kHz. Due to the influence of intracavity loss in the cavity-enhanced quantum memory system, the observed values are worse than the ideal system. From Fig. S1, we can see that the smaller intracavity loss is, the better the memory efficiency is. The black star depicts the experimental result of $\eta(T_0) = 78 \pm 1\%$ where the transmissivity of the input-output mirror T is 0.30 and the intracavity loss L is about 0.02.

Supplementary Note 4 - Analysis of the memory fidelity of cavity-enhanced quantum memory

In the quantum memory, the fidelity $F = \{Tr[(\hat{\rho}_1^{1/2}\hat{\rho}_2\hat{\rho}_1^{1/2})^{1/2}]\}^2$, which describes the overlap of input state with the stored-and-retrieved state, quantifies its performance^{1,2}. The fidelity for Gaussian input and stored-and-retrieved states can be obtained by the covariance matrices $A_{1(2)} = 4 \begin{pmatrix} \langle \Delta^2 \hat{x} \rangle_{1(2)} & 0 \\ 0 & \langle \Delta^2 \hat{p} \rangle_{1(2)} \end{pmatrix}$ and mean amplitudes $\alpha_{1(2)} = \begin{pmatrix} \alpha_{x1(2)} \\ \alpha_{p1(2)} \end{pmatrix}$ of the input and stored-and-retrieved signal mode, which is³

$$F = \frac{2}{\sqrt{\Delta + \sigma} - \sqrt{\sigma}} \exp[-\varepsilon^T (A_1 + A_2)^{-1} \varepsilon], \quad (\text{S1})$$

where $\varepsilon = \alpha_2 - \alpha_1$, $\Delta = \det(A_1 + A_2)$, $\sigma = (\det A_1 - 1)(\det A_2 - 1)$.

The measured data of quadrature components are substituted in Eq. (S1) to calculate the fidelity. In this way, the memory fidelity of the input and stored-and-retrieved states of signal mode in quantum memory is obtained. The different memory efficiencies in table 1 are obtained by changing the cell temperature, which are estimated with the photoreceiver detector D1 measurement of the input and stored-and-retrieved optical modes.

¹ Nha, H. & Carmichael, H. J. Distinguishing two single-mode Gaussian states by homodyne detection: An information-theoretic approach. *Phys. Rev. A* **71**, 032336 (2005).

² Scutaru, H. Fidelity for displaced squeezed thermal states and the oscillator semigroup. *J. Phys. A: Math. Gen.* **31**, 3659 (1998).

³ Su, X.-L., Hao, S.-H., Deng, X.-W., Ma, L.-Y., Wang, M.-H., Jia, X.-J., Xie, C.-D. & Peng, K.-C. Gate sequence for continuous variable one-way quantum computation. *Nat. Commun.* **4**, 2828 (2013).